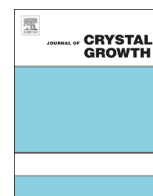




ELSEVIER

Contents lists available at ScienceDirect

Journal of Crystal Growth

journal homepage: www.elsevier.com/locate/jcrysgr

Studies on the structure, growth and characterization of morpholinium perchlorate single crystals



A. Arunkumar, P. Ramasamy*

Centre for Crystal Growth, SSN college of Engineering, Kalavakkam 603110, India

ARTICLE INFO

Article history:

Received 2 April 2013

Received in revised form

30 June 2013

Accepted 1 October 2013

Communicated by K. Jacobs

Available online 16 November 2013

Keywords:

A1. Solubility

A2. Growth from solutions

B1. Organic compounds

B2. Nonlinear optic materials

ABSTRACT

Morpholinium perchlorate, an organic nonlinear optical material was synthesized and the crystals were grown by the slow evaporation solution growth technique. Single crystal X-ray diffraction study revealed that the grown crystal belongs to orthorhombic system with space group of $P2_12_12_1$. The structure of the compound was also confirmed by ^1H NMR studies. The Fourier transform infrared analysis was used to identify the various functional groups present in the title compound. The UV–visible absorption spectrum was recorded to study the optical transmittance in the range from 200 to 1100 nm. The optical band gap, reflectance, refractive index (n), extinction coefficient and electric susceptibility were calculated using transmittance data. The mechanical stability of the grown crystal was studied by Vickers's micro hardness test. The PL spectrum of the title compound shows red emission at 648 nm.

© 2013 Elsevier B.V. All rights reserved.

1. Introduction

The technological society of optoelectronics and photonics has created more attention on organic optical materials. Nowadays organic and semiorganic NLO materials are emerging as an alternative to inorganic materials because of their efficient molecular nonlinearity over a broad frequency range, low cost, low refractive index, low dielectric constant, inherent synthetic flexibility, moderate optical damage density, fast response with the better process ability and ease of fabrication into devices. The organic nonlinear optical materials generally have the larger second order nonlinear optical coefficient and hence they are being used in many applications such as second harmonic generation, sum frequency generation, THz wave generation, optical parametric oscillators, etc., [1–5]. Researches to explore the third order nonlinear optical phenomena in organic and inorganic single crystals have received limited attention compared to second order nonlinear optical materials. For the past ten years, the third order nonlinear optical materials from the organometallic, organic, inorganic and semi organic single crystalline compounds have received great deal of attention due to their potential applications in all optical switching, optical limiters, optical information storage, all optical logic gates, laser radiation protection etc., [6,7]. Crystals of organic salts are often colorless, transparent, inexpensive to produce

and easy to grow [8]. Morpholine is colorless, oily and volatile in nature having great importance in industrial purposes [9]. Molecular ionic simple complex crystals like perchlorate with Morpholine (of ratio 1:1), shows nonlinear optical physical properties unique to the crystal structure. The distinct features of molecular ionic crystal give empathizing correlation between the crystal packing and physical properties. This initiated many researchers to synthesize and to grow the newly designed molecular ionic crystals. In this paper we present the structure of morpholinium perchlorate (MP) at room temperature, crystal growth and its characterization.

2. Experiment

The title material MP was synthesized by the chemical reaction of commercially available Morpholine (Merck) with Perchloric acid (SRL), taken in the stoichiometric ratio 1:1 by dissolving in the mixture of (1:1) ethanol and deionized water. The chemical reaction is shown in Fig. 1. Stoichiometrically calculated amounts of the materials were transferred into a beaker and dissolved in ethanol and deionized water which is stirred well with the help of a magnetic stirrer to make a homogeneous solution of the material at a temperature of 50 °C for a proper chemical reaction. The white precipitate was obtained after two hours. The precipitate is allowed to dry. The dried salt was collected and used for the further growth of MP. The synthesized material was purified by the repeated recrystallization process. The dried precipitate was dissolved using the same solvent. But the crystallization did not occur in this solution as it has high viscosity and low pH value. The selection of solvent is

* Corresponding author. Tel.: +91 9283105760; fax: +91 44 27475166.

E-mail addresses: ramasamp@ssn.edu.in,
proframasamy@hotmail.com (P. Ramasamy).

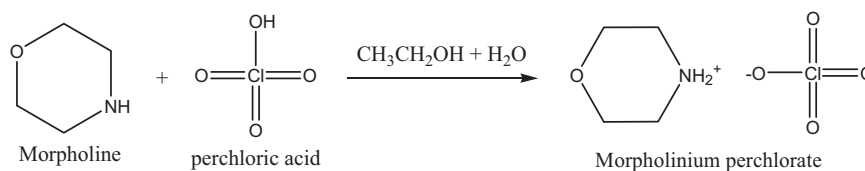


Fig. 1. Reaction scheme of MP.

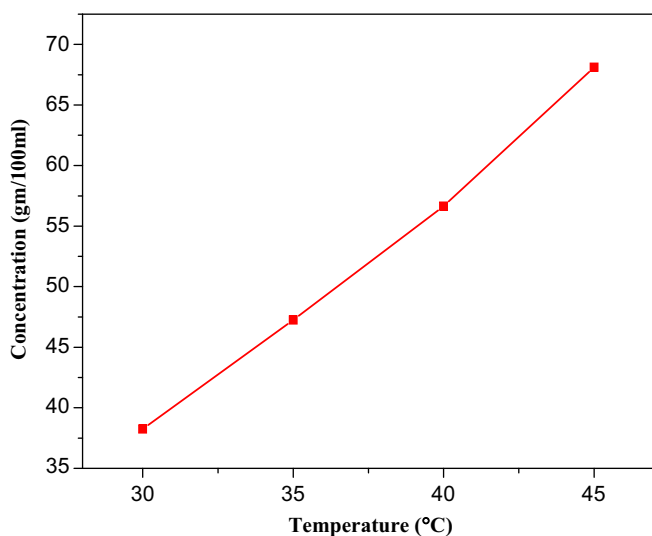


Fig. 2. Solubility diagram of MP.



Fig. 3. As grown single crystals of morpholinium perchlorate (MP).

important to grow good quality single crystals of considerable size. The solubility test can be performed to choose the solvent for crystal growth. The solubility was measured by taking excess amount of MP in the solvent and it is continuously stirred to achieve uniform concentration over the entire volume of the solution. Solubility curve for MP was determined by using acetone as a solvent in the temperature range from 30 to 45 °C with the interval of 5 °C. The studies were carried out in a constant-temperature water bath with a cryostat facility with an accuracy of ± 0.01 K. MP exhibits a positive solubility – temperature gradient in acetone solution. The solubility almost increases linearly with the increase of temperature. Fig. 2 depicts the solubility curve of MP. The obtained dried precipitate was dissolved using acetone and then allowed to evaporate at room temperature to yield the crystalline powder salt of MP. The well-defined single crystals of MP were harvested from mother solution after a growth period of 45 days. The grown single crystals of MP are shown in Fig. 3

3. Characterization

As grown MP crystals have been subjected to various characterization studies to analyze the structural, thermal, optical and mechanical properties. The single crystal X-ray diffraction measurements were done using a Bruker AXS Kappa APEX II single crystal CCD diffractometer equipped with graphite-monochromated MoK α radiation ($\lambda = 0.71073$ Å) at room temperature with a crystal of dimension $0.35 \times 0.25 \times 0.2$ mm³. Accurate unit cell parameters were determined from the reflections of 36 frames measured in three different crystallographic zones. The data collection, data reduction and absorption correction were performed by APEX2, SAINT-plus and SADABS program using SHELXL-97 [10]. The structure was solved by direct methods procedure and the non-hydrogen atoms were subjected to anisotropic refinement by full-matrix least squares on F² using SHELXL-97 program [11]. The positions of all the hydrogen atoms were identified from difference electron density map, and they were constrained to ride on the corresponding non-hydrogen atoms. The hydrogen atom bound to carbon atoms were constrained to a distance of C–H = 0.97 Å and $U_{\text{iso}}(\text{H}) = 1.2 U_{\text{eq}}(\text{C})$. The final refinement converges to an R -values of $R_1 = 0.0485$ and $WR_2 = 0.1330$. The ORTEP drawing was performed with the ORTEP3 program [12]. The crystallographic refinement parameters are listed in Table 1. The possible hydrogen bonds observed in the structure are listed in Table 2. The crystalline perfection of the grown single crystals was characterized by HRXRD by employing a multicrystal X-ray diffractometer developed at NPL [13]. The well-collimated and monochromated MoK α_1 beam obtained from the three monochromator Si crystals set in dispersive (+, –, –) configuration has been used as the exploring X-ray beam. The specimen crystal is aligned in the (+, –, –, +) configuration. Due to dispersive configuration, though the lattice constant of the monochromator crystal(s) and the specimen are different, the unwanted dispersion broadening in the diffraction curve (DC) of the specimen crystal is insignificant. The specimen can be rotated about the vertical axis, which is perpendicular to the plane of diffraction, with minimum angular interval of 0.4° . The rocking or diffraction curves were recorded by changing the glancing angle (angle between the incident X-ray beam and the surface of the specimen) around the Bragg diffraction peak position θ_B (taken as zero for the sake of convenience) starting from a suitable arbitrary glancing angle and ending at a glancing angle after the peak so that all the meaningful scattered intensities on both sides of the peak are included in the diffraction curve. The DC was recorded by the so-called ω scan wherein the detector was kept at the same angular position $2\theta_B$ with wide opening for its slit. This arrangement is very appropriate to record the short range order scattering caused by the defects or by the scattering from local Bragg diffractions from agglomerated point defects or due to low angle and very low angle structural grain boundaries [14]. Before recording the diffraction curve to remove the non-crystallized solute atoms which remained on the surface of the crystal and the possible layers which may sometimes form on the surfaces on crystals grown by solution methods [15] and also to ensure the surface planarity, the specimen was first lapped and chemically etched in a non-preferential etchant of water and acetone mixture in 1:2 volume ratio. The FTIR spectrum of MP crystals was recorded in the range 4000–400 cm⁻¹

Table 1
Crystal data and structure refinement for MP.

Empirical formula	C ₄ H ₁₀ ClNO ₅
Formula weight	187.58
Temperature	293(2) K
Wavelength	0.71,073 Å
Crystal system, space group	Orthorhombic, P2 ₁ 2 ₁ 2 ₁
Unit cell dimensions	$a=8.2802(4)$ Å $\alpha=90^\circ$ $b=9.7730(6)$ Å $\beta=90^\circ$ $c=9.5591(5)$ Å $\gamma=90^\circ$
Volume	1163.3(4) Å ³
Z, Calculated density	4, 1.611 Mg/m ³
Absorption coefficient	0.472 mm ⁻¹
F(000)	392
Crystal size	0.35 × 0.30 × 0.20 mm
Theta range for data collection	2.98–32.32°
Limiting indices	$-12 \leq h \leq 8$, $-13 \leq k \leq 14$, $-12 \leq l \leq 14$
Reflections collected/unique	10,043/2707 [R(int)=0.0325]
Completeness to theta=25.00	99.9%
Absorption correction	Semi-empirical from equivalents
Max. and min. transmissions	0.8912 and 0.8523
Refinement method	Full-matrix least-squares on F ²
Data/restraints/parameters	2707/136/147
Goodness-of-fit on F ²	1.054
Final R indices [I > 2σ(I)]	R1=0.0485, wR2=0.1330
R indices (all data)	R1=0.0732, wR2=0.1595
Largest diff. peak and hole	0.678 and -0.438 e Å ⁻³

Table 2
The possible hydrogen bonds observed in the structure of MP.

D–H...A	d(D–H)	d(H...A)	d(D...A)	<(DHA)
N(1)–H(1A)...O(4)#1	0.90	2.02	2.773(6)	140.0
N(1)–H(1A)...O(3)#2	0.90	2.50	3.057(12)	120.2
N(1)–H(1B)...O(5)#2	0.90	2.01	2.888(2)	166.1
C(1)–H(1C)...O(1)#3	0.97	2.60	3.446(8)	146.0
C(1)–H(1D)...O(2)#4	0.97	2.57	3.507(7)	163.3
C(3)–H(3A)...O(2)#5	0.97	2.58	3.485(6)	154.7
C(2)–H(2B)...O(3)#6	0.97	2.44	3.364(10)	159.9

Symmetry transformations used to generate equivalent atoms: #1 $x, y, z-1$, #2 $x-1/2, -y+1/2, -z+1$, #3 $x+1/2, -y+1/2, -z+1$, #4 $-x+1/2, -y, z-1/2$, #5 $-x+1, y+1/2, -z+3/2$, #6 $-x+1, y-1/2, -z+3/2$.

employing a JASCO FT-IR 410 spectrometer by the KBr pellet method to study the functional groups in sample. In the present investigation, the ¹H spectra of MP was recorded using acetone as solvent on a Bruker 300 MHz (Ultra shield) TM instrument at 23 °C (300 MHz for ¹H NMR) to confirm the molecular structure. Optical transmittance was studied at room temperature using a PerkinElmer Lambda 35 UV–vis spectrometer in the region 200–1100 nm. Fluorescence of the MP crystal was studied in the emission range of 200–750 nm using JASCO fluorimeter.

4. Results and discussions

4.1. Single crystal X-ray diffraction studies

The title compound MP crystallizes in orthorhombic space group P2₁2₁2₁. The structure of morpholinium perchlorate in the low-temperature form (100 K) was previously reported [16] in non-standard unit cell parameter settings. The previously reported cell parameters values are “ $a=8.1515$ (3) Å, $b=9.5435$ (4) Å, $c=28.9022$ (12) Å and $V=2248.41$ (16) Å³”, with three independent formula units in the unit cell. The crystal structure shows pseudo inversion centre. The structure was partially resolved in centrosymmetric space group Pnma with half anions and cations in the asymmetric form and with high R-value. But the systematic absent

reflections show the absence of Pnma symmetry. Hence the structure is refined finally in P2₁2₁2₁ space group. The present unit cell is indexed to a standard setting of “ $a=8.2802(4)$ Å, $b=9.7730(6)$ Å, $c=9.5591(5)$ Å and $V=773.55(7)$ Å³”, whose c-axis is one third of the previously reported structure with only one formula unit in the unit cell. In MP the perchlorate anion is severely disordered in positions one and two with refined site occupancies of 0.560 (3) and 0.440 (3) respectively. The bond lengths of the minor component were made similar to the major component using similarity restraints with s.u 0.01 Å and the atomic displacement parameters of the disordered components were made similar using suitable similarity restraints. The molecular structure of MP is shown in Fig. 4. The molecular packing in the crystal is primarily decided by N–H...O and C–H...O hydrogen bonds. The bonds N1–H1A...O4, N1–H1A...O3 and N1–H1B...O5 inter connect the anion and the cation to form a molecular sheet parallel to (010) plane. The presence of C–H...O hydrogen bond in the C1–H1C...O1 molecular sheet stabilizes the network and is shown in Fig. 5. Parallely stacking molecular (010) sheets along the b-axis is further linked through C1–H1D...O2, C3–H3A...O2 and C2–H2B...O3 hydrogen bond to generate a three dimensional hydrogen bond networks which constitute the molecular packing in the crystalline solid. The pseudo chain formation of morpholinium perchlorate is shown in Fig. 6. CCDC no. 910879 contains the supplementary crystallographic data for this paper. These data can be obtained free of charge via www.ccdc.cam.ac.uk/data-request/cif, by e-mailing data-request@ccdc.com.ac.uk or by contacting the Cambridge crystallographic data centre, 12 Union Road, Cambridge CB21 EZ, UK; fax: +44 1223 336033.3.2.

4.2. High resolution X-ray diffraction studies

Fig. 7 shows the DC recorded for a typical MP single crystal using (112) diffracting planes in symmetrical geometry using MoKα₁ radiation. On close observation one can realize that the curve is not a single peak. On deconvolution of the diffraction curve, it is clear that the curve contains an additional peak which is 13'' away from the main peak. The additional peak corresponds to an internal structural low angle grain boundary. For better understanding, the schematic of a structural grain boundary is given in the inset of Fig. 7. As seen in the inset two regions of the crystal are misoriented by a finite angle α also known as tilt angle. Tilt angle may be defined as the misorientation angle between the two crystalline regions on both sides of the structural grain boundary. The two regions may be perfect. If the value of α is $\leq 1'$, we may call it as very low angle boundary. If $\alpha > 1'$ but less than a deg, we call it as low angle boundary. For more details of such structural grain boundaries including their effect on physical properties, reference is made available elsewhere [17,18]. The angular separation between the two peaks gives the tilt angle α . The tilt angle for the very low angle boundary is 13'' with respect to the main crystal block. The FWHM (full width at half maximum) of the main peak and the boundary is respectively 17 and 12''. The low FWHM values of main crystal and the very low angle boundary indicate that the crystalline perfection of the specimen is quite good. This type of structural defects is probably due to strains developed in the crystal during the growth process due to thermal/mechanical fluctuations. Another cause could be the fast growth [18]. It may be mentioned here that such minute defects could be detected with well resolved peaks in the diffraction curve only because of the high-resolution of the diffractometer, characterized by very low values of wavelength spread i.e. $\Delta\lambda/\lambda$ and horizontal divergence for the exploring or incident beam, which are respectively around 10^{-5} and much less than 3'' of the multi crystal X-ray diffractometer used in the present studies. Such defects may not influence much on the NLO properties. However,

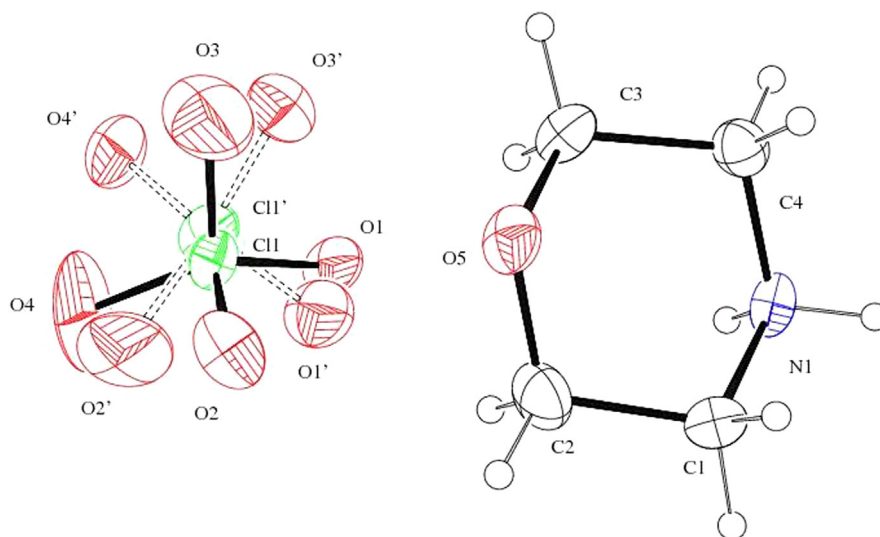


Fig. 4. Molecular structure of MP.

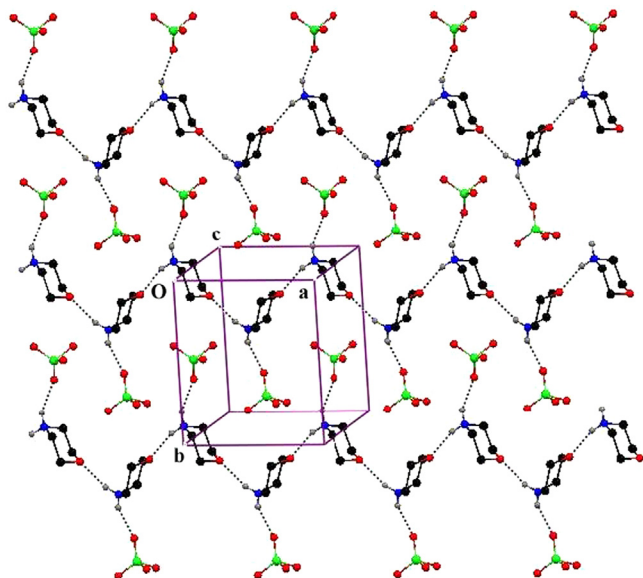


Fig. 5. Sheet of MP.

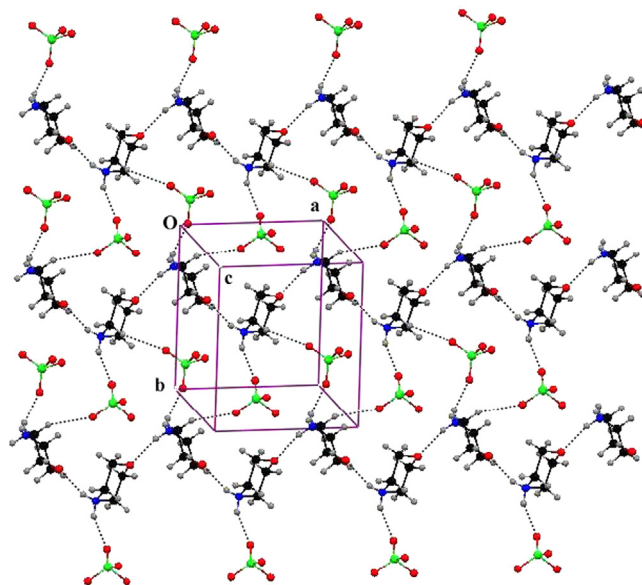


Fig. 6. Chain formation of MP.

a quantitative analysis of such unavoidable defects is of great importance, particularly in case of phase matching applications as explained in the recent article [19].

4.3. FT-IR spectral analysis

Fig. 8 shows the FTIR spectrum of MP. The symmetric and asymmetric stretching vibrations of NH_2^+ cation occurred at 3415 and 3282 cm^{-1} . The CH asymmetric and symmetric vibrations of morpholinium ring are observed at 2945 and 2865 cm^{-1} . The stretching vibration of NH_2^+ cation occurred at 2449 cm^{-1} . The C–O–C stretching vibrations of morpholinium ring occurred at 1105 (asymmetric) and 1035 (symmetric) cm^{-1} . The C–N in-plane and out of plane bending vibrations occurred at 940 and 525 cm^{-1} . The stretching vibrations of chlorate counter anion occurred at 2203 , 2163 and 1144 cm^{-1} . The C–N stretching vibration occurred at 1315 cm^{-1} . The NH bending vibration occurred at 1574 cm^{-1} . The N–H wagging vibration occurred at 691 cm^{-1} . The CH bending vibration is observed at 895 cm^{-1} .

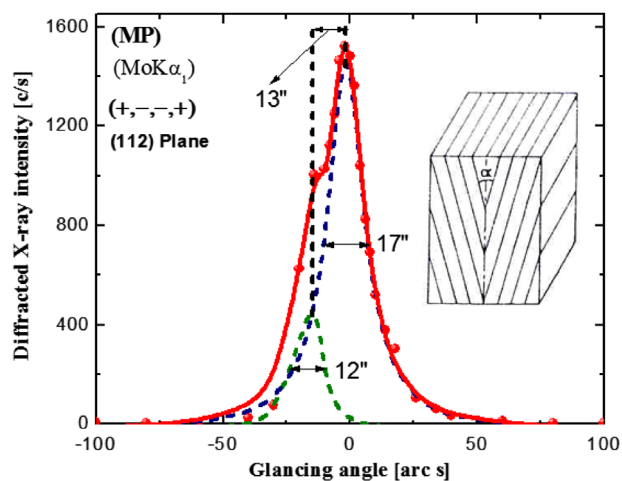


Fig. 7. High resolution X-ray diffraction curve of MP.

Hence the spectrum shows the characteristic absorptions of both morpholine and perchloric acid as morpholinium perchlorate.

4.4. NMR spectral analysis

The NH proton signal is observed at 2.7 ppm. The peak at 3.5 ppm is assigned to CH₂ protons ortho to NH group. The signal at 3.95 ppm is assigned to CH₂ protons meta to NH group. The ¹H NMR spectrum of MP is shown in Fig. 9.

4.5. UV-vis-NIR spectral analysis

Fig. 10 shows the UV-vis spectrum of MP crystal. The crystal has sufficient transmission in the UV and visible region. The cut-

off wavelength of MP crystal was found to be 215 nm and the absorption at 279 nm was due to the promotion of an electron from a 'non-bonding' (lone-pair) n orbital to an 'anti-bonding' π^* orbital designated as π^* ($n \rightarrow \pi^*$) and no characteristic absorption was observed in the entire visible region. The dependence of optical absorption coefficient with the photon energy helps to study the band structure and the type of transition of the electron. The absorption coefficient (α) and the optical parameters such as refractive index (n), reflectance (R) and extinction coefficient (K) have been determined from the transmission (T) spectrum based on the following relation:

$$\alpha = \frac{2.3026}{t} \log(1/T) \quad (1)$$

where T is transmittance, ' t ' is the thickness of the crystal, ' α ' is

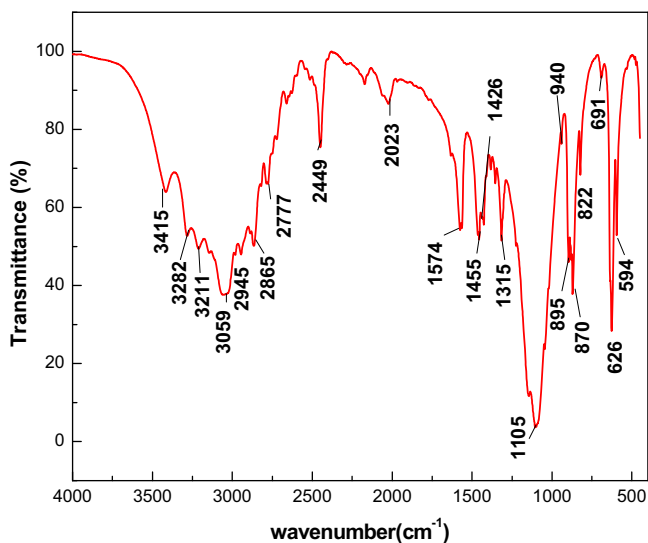


Fig. 8. FTIR spectrum of MP.

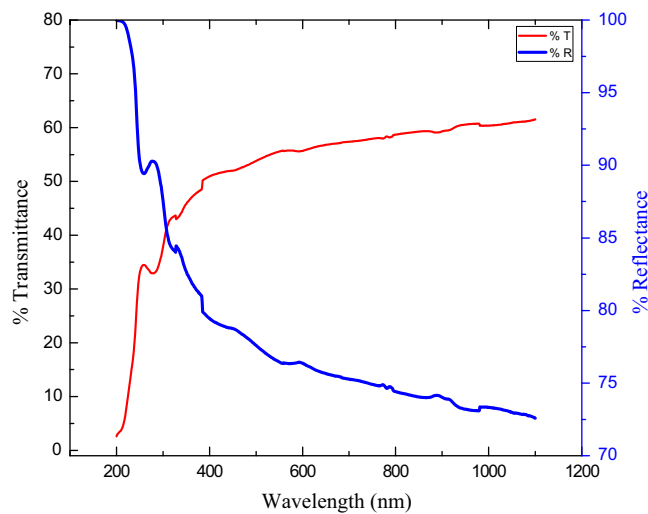


Fig. 10. Transmittance and reflectance spectrum of MP crystal.

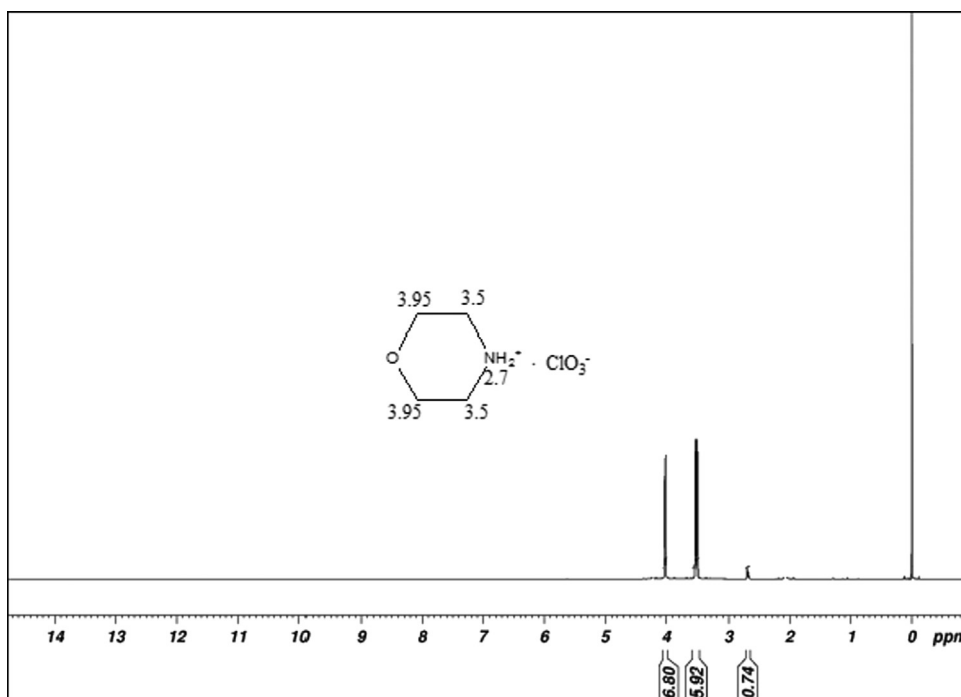


Fig. 9. ¹H NMR spectrum of MP.

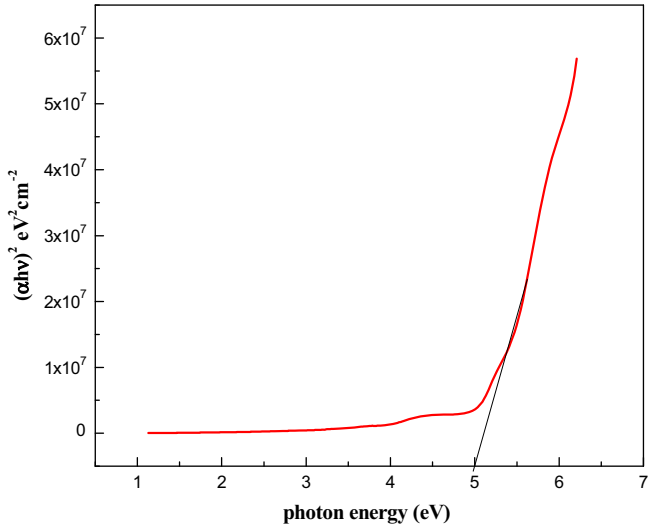


Fig. 11. Plot of $(\alpha h\nu)^2$ vs. photon energy.

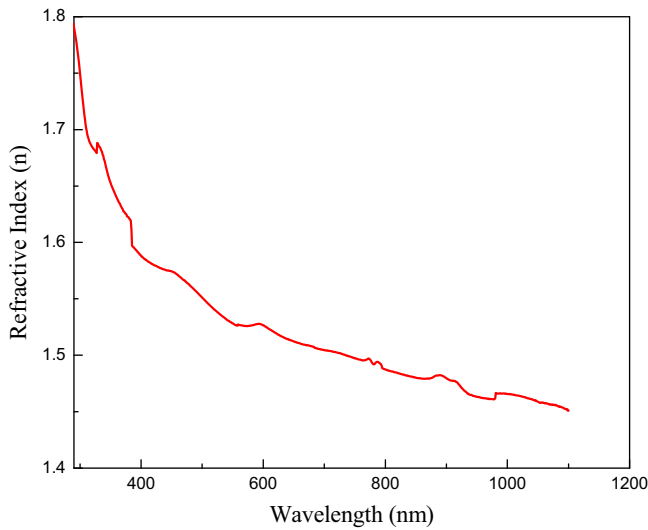


Fig. 12. Plot of refractive index vs. wavelength.

related to the extinction coefficient K by

$$K = \frac{\alpha\lambda}{4\pi} \quad (2)$$

The reflectance (R) in terms of the absorption coefficient and refractive index (n) can be derived from the relations

$$R = \frac{\exp(-\alpha t) \pm \sqrt{\exp(-\alpha t)T - \exp(-3\alpha t)T + \exp(-2\alpha t)T^2}}{\exp(-\alpha t) + \exp(-2\alpha t)T} \quad (3)$$

$$n = \frac{-(R+1) \pm 2\sqrt{R}}{(R-1)} \quad (4)$$

In the high photon energy region, the energy dependence of absorption coefficient suggests the occurrence of direct band gap of the crystal obeying the following equation for high photon energies ($h\nu$) [20]

$$(\alpha h\nu)^2 = A(E_g - h\nu) \quad (5)$$

where E_g is the optical band gap of the crystal and A is a constant. The band gap of the crystal was evaluated by plotting $(\alpha h\nu)^2$ versus $h\nu$ as shown in Fig. 11 and it was found to be 5 eV. The wide band gap of the MP crystals confirms the large transmittance in the visible region. Fig. 12 represents the variation of refractive index with respect to wavelength (215–1100 nm) respectively. The estimated refractive index (n) of MP crystal from the graph is 1.41 at 600 nm.

From the optical constants, the electric susceptibility χ_c can be calculated according to the relation [21]

$$\epsilon_r = \frac{\epsilon_0 + 4\pi\chi_c}{4\pi} = n^2 - K^2 \quad (6)$$

$$\chi_c = \frac{(n^2 - K^2 - \epsilon_0)}{4\pi} \quad (7)$$

where ϵ_0 is the dielectric constant in the absence of any contribution from free carriers. The estimated electric susceptibility (χ_c) is found to be 0.19 at 600 nm.

The real and imaginary dielectric constants, ϵ_r and ϵ_i can be calculated from the following relations [22]:

$$\epsilon_r = n^2 - K^2 \text{ and } \epsilon_i = 2nK \quad (8)$$

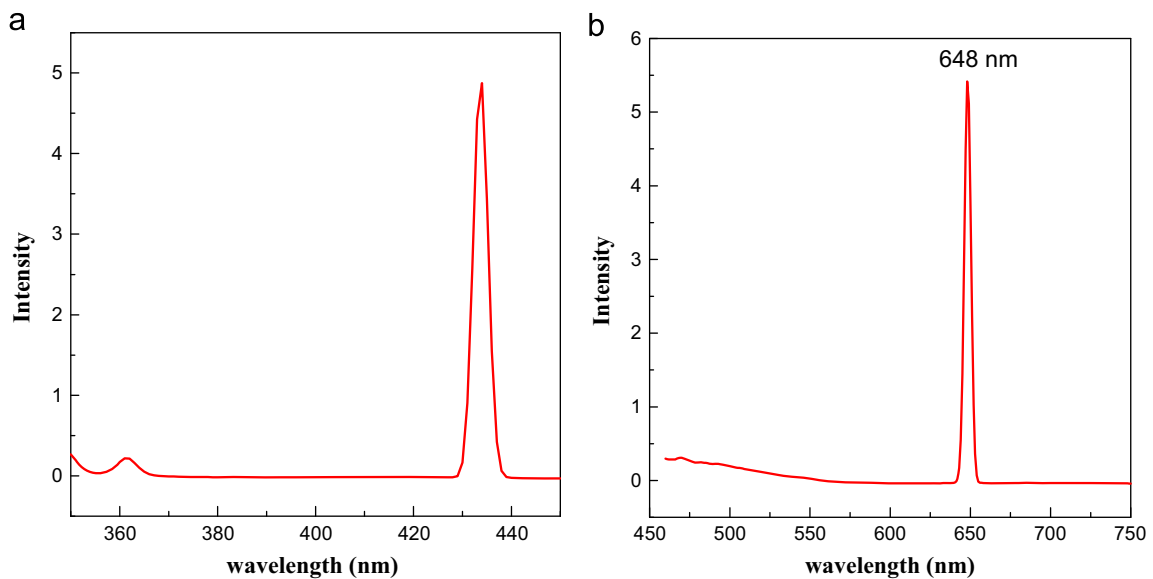


Fig. 13. (a) Excitation and (b) emission spectra of MP.

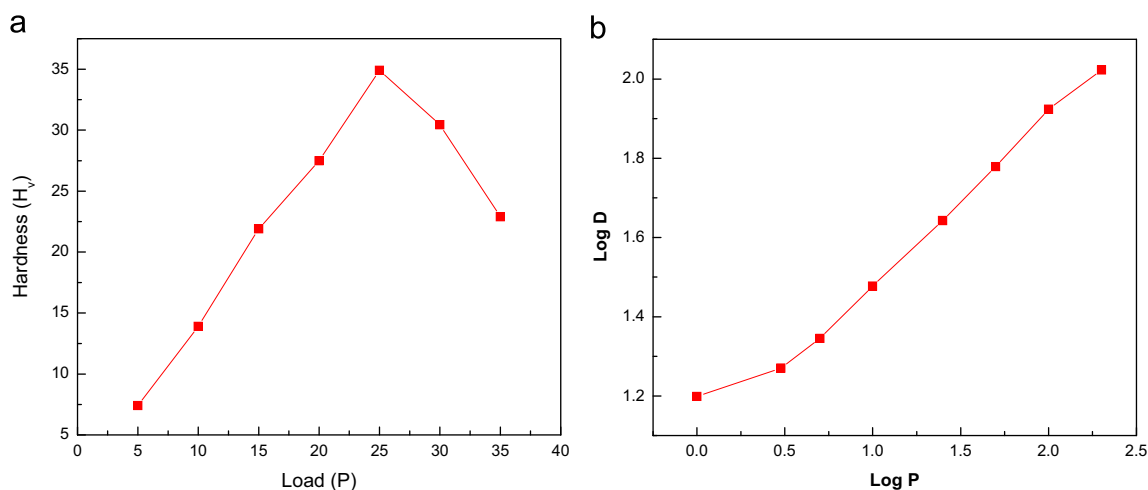


Fig. 14. (a) Load (P) vs. Hardness number (H_v) and (b) Plot of $\log P$ vs. $\log D$ of MP.

The real ϵ_r and imaginary ϵ_i dielectric constants at 600 nm were found to be 2.40 and 2.5×10^{-5} respectively.

4.6. Fluorescence analysis

The excitation spectrum was recorded in the range of 220–350 nm and the sample was excited at 434 nm. The emission spectrum was measured in the range of 450–750 nm. The excitation and emission spectrum of MP is given in Fig. 13 (a) and (b). Sharp peak was observed at 648 nm and it shows the characteristic nature of red emission. The full width at half maximum of emission peak is 4.78 nm which shows that the quality of the crystal is good.

4.7. Mechanical properties

Microhardness studies were conducted for the loads in the range 5–35 g. Vickers's hardness (H_v) number increases initially with load up to 25 g (Fig. 14(a)) and cracks were observed beyond 25 g. This type of load dependent variation of hardness is termed as reverse indentation size effect. At low loads, the indenter penetrates only the top surface layers generating dislocations, which results in the increase of hardness in this region. The load independence of hardness at higher loads can be attributed to the mutual interaction or rearrangement of dislocations [23]. The relation between load and the size of indentation can be correlated using Meyer's law, $P = k_1 d^m$, where k_1 is a constant and ' m ' is the Meyer's index. Fig. 14 (b) shows the plot between $\log P$ and $\log D$. From the slope of graph the work hardening coefficient (m) was calculated and it is found to be 2.7 which indicates that MP crystal belongs to soft material category.

4.8. Nonlinear optical studies

In order to know its second order nonlinear optical property of MP crystal, the Kurtz Perry powder technique was used. Complete absence of second order NLO property was observed from the result and it is due to the pseudo inversion centre present in the crystal packing and pseudo symmetry present in the structure of MP which is similar to the structure of L-Histidinium sulfate [24].

5. Conclusion

Simple ionic morpholinium perchlorate crystal was synthesized and bulk crystals were grown using the slow evaporation

solution growth technique. The structure was solved with standard unit cell parameter settings at room temperature. The presence of functional groups in the MP crystal was confirmed using FTIR studies. The crystalline perfection of the grown crystal was fairly good confirmed by high resolution X-ray diffraction. The optical behavior was evaluated by UV-vis-NIR and photoluminescence analyses which substantiate the suitability of MP for optoelectronic applications. The optical band gap, refractive index and electric susceptibility were calculated from the linear optical data. From microhardness measurements it is observed that the MP comes under the soft materials category. Red emission was observed in the PL spectrum of crystal.

Acknowledgments

The authors thank SAIF, IIT Madras, Chennai for recording NMR spectrum, and single crystal data collection. The authors thank Dr. G. Bhagavannarayana, NPL, New Delhi for HRXRD studies.

Appendix A. Supplementary material

Supplementary data associated with this article can be found in the online version at <http://dx.doi.org/10.1016/j.jcrysgro.2013.10.005>.

References

- [1] D.S. Chemla, J. Zyss (Eds.), Academic Press, New York, 1987.
- [2] L.R. Dalton, P.A. Sullivan, B.C. Olbricht, D.H. Bale, J. Takayesu, S. Hammond, H. Rommel, B.H. Robinson, *Tutorials in Complex Photonic Media*, SPIE, Bellingham, WA, 2007.
- [3] R.W. Munn, C.N. Ironside, *Principles and Applications of Nonlinear Optical Materials*, Chapman & Hall, London, 1993.
- [4] M. Thakur, J. Xu, A. Bhowmik, L. Zhou, *Appl. Phys. Lett.* 74 (1999) 635–637.
- [5] T. Kaino, B. Cai, K. Takayama, *Adv. Funct. Mater.* 12 (2002) 599–603.
- [6] M. Somac, A. Somac, B.L. Davies, M.G. Humphery, M.S. Wong, *Opt. Mater.* 21 (2003) 485–488.
- [7] L.V. Natarajan, R.L. Sutherland, V.P. Tondiglia, T.J. Bunning, W.W. Adams, *J. Nonlinear Opt. Phys. Mater.* 5 (1996) 89–98.
- [8] P.V. Dhanaraj, N.P. Rajesh, J. Kalyana Sundar, S. Natarajan, G. Vinitha, *Mater. Chem. Phys.* 129 (2011) 457–463.
- [9] P. Szklarz, M. Owczarek, G. Bator, T. Lis, K. Gatner, R. Jakubas, *J. Mol. Struct.* 929 (2009) 48–57.
- [10] Bruker–Nonius AXS, APEX2 and SAINT, Bruker–Nonius AXS, Madison, Wisconsin, USA, 2004.
- [11] G.M. Sheldrick, *Acta Cryst.* A64 (2008) 112–122.
- [12] L.J. Farrugia, ORTEP-3 program for molecular drawing, *J. Appl. Cryst.* 30 (1997) 561–565.
- [13] Krishan Lal, G. Bhagavannarayana, *J. Appl. Cryst.* 22 (1989) 209–215.
- [14] G. Bhagavannarayana, S.K. Kushwaha, *J. Appl. Cryst.* 43 (2010) 154–162.

- [15] G. Bhagavannarayana, S. Parthiban, Subbiah Meenakshisundaram, *J. Appl. Cryst.* 39 (2006) 784–790.
- [16] Mikhail S. Grigoriev, Konstantin E. German, Alesia Ya. Maruk, *Acta Cryst.* E64 (2008) o390–o401.
- [17] G. Bhagavannarayana, R.V. Ananthamurthy, G.C. Budakoti, B. Kumar, K.S. Bartwal, *J. Appl. Cryst.* 38 (2005) 768–771.
- [18] G. Bhagavannarayana, P. Rajesh, P. Ramasamy, *J. Appl. Cryst.* 43 (2010) 1372–1376.
- [19] G. Bhagavannarayana, B. Riscob, Mohd Shakir, *Mater. Chem. Phys.* 126 (2011) 20–23.
- [20] A. Ashour, N. El-Kadry, S.A. Mahmoud, *Thin Solid Films* 269 (1995) 111–120.
- [21] J. Tauc, R. Grigorovici, A. Vancu, *Phys. Status Solidi B* 15 (1966) 627–637.
- [22] V. Gupta, A. Mansingh, *J. Appl. Phys.* 80 (1996) 1063–1073.
- [23] J.H. Gong, Y. Li, *J. Mater. Sci.* 35 (2000) 209–213.
- [24] H.A. Petrosyan, H.A. Karapetyan, A.K. Atanesyan, A.M. Petrosyan, *J. Mol. Struct.* 963 (2010) 168–174.